[19] Trevizol 2016 Trigeminal nerve stimulation (TNS) for posttraumatic stress disorder and major depressive disorder: An open-label proof-of-concept trial
[20] Fallgatter 2003 Far field potentials from the brain stem after transcutaneous vagus nerve stimulation.
[21] Stavrakis 2015 Low-level transcutaneous electrical vagus nerve stimulation suppresses atrial fibrillation.
[22] Fang 2015 Transcutaneous Vagus Nerve Stimulation Modulates Default Mode Network in Major Depressive Disorder.
[23] Rong 2016 Effect of transcutaneous auricular vagus nerve stimulation on major depressive disorder- a nonrandomized controlled pilot study
[24] Huston 2007 Transcutaneous vagus nerve stimulation reduces serum high mobility group box 1 levels and improves survival in murine sepsis
[25] Ellrich 2011 Inhibition Of Pain Processing By Transcutaneous Vagus Nerve Stimulation (Abstract & Poster)
[26] Ellrich 2011 Analgesic Effects of Transcutaneous Vagus Nerve Stimulation (Abstract)
[27] Nitsche & Paulus 2000 Excitability changes induced in the human motor cortex by weak transcranial direct current stimulation
[28] Bikson 2016 Safety of Transcranial Direct Current Stimulation- Evidence Based Update 2016

PROCEEDINGS #21. INTRACRANIAL VOLTAGE RECORDING DURING TRANSCRANIAL DIRECT CURRENT STIMULATION (TDCS) IN HUMAN SUBJECTS WITH VALIDATION OF A STANDARD MODEL

Zeinab Esmaeilpour [1], Matija Milosevic [2,3], Kleber Azevedo [4], Niranjan Khadka [1], Jessie Navarro [4], Andre Brunoni [5], Milos R. Popovic [2,3], Marom Bikson [1], Erich Talamoni Fonoff [6]. [1] *Department of Biomedical Engineering, the City Collage of New York, NY, USA;* [2] *Institute of Biomaterials and Biomedical Engineering, University of Toronto, ON, Canada;* [3] *Rehabilitation Engineering Laboratory, Toronto Rehabilitation Institute - University Health Network, Toronto, ON, Canada;* [4] *Division of Functional Neurosurgery of Institute of Psychiatry of Hospital das Clinicas of University of São Paulo medical School, Brazil;* [5] *Institute of Psychiatry of Hospital das Clinicas of University of São Paulo medical School, Brazil;* [6] *Department of Neurology and Division of Functional Neurosurgery of Institute of Psychiatry of Hospital das Clinicas of University of São Paulo medical School, Brazil*

1. Abstract and Introduction

During transcranial direct current stimulation (tDCS) weak (1-2 mA) currents are applied across the head, producing low-intensity electric fields in the brain with the intention of modulating neuronal function. For any application of tDCS spanning cognitive neuroscience and neuropsychiatric therapies [1], understanding the amount of current delivered to the brain and the resulting electric field (in V/m) produced is thus important. In animal studies, direct current (DC) electric fields as low as 0.2-1.0 V/m influence neuronal excitability and plasticity [2, 3]. Since measurement of electric field in human is difficult to implement, high-resolution finite element head models [4] have been used to predict brain current flow during tDCS [5] - with many reports adapting a standard (S#) head [6-8]. There have been previous attempts to validate computational model predictions indirectly with scalp electrodes [9] and neurophysiology [10] during tDCS, as well as directly using intra-cranial electrodes, but not with DC stimulation [11, 12]. In this pilot study, DC voltage was measured using deep brain stimulation (DBS) and epidural lead electrodes during application of tDCS in human subjects. The results were evaluated against a standard (S#) head model. The model predictions of voltage produced across cortical (epidural) electrodes were consistent with recorded data, while subcortical (DBS) voltages were sensitive to conductivity assigned to subcortical structures.

2. Methods

Three subjects were recruited for the study: subject #1 - 59 years old male, two DBS electrodes implanted bilaterally (3387, Medtronic Inc., USA) in nucleus accumbens (NA), subject #2 - 51 years old male, two DBS electrodes implanted bilaterally (6145, St. Jude Medical Inc., USA) in subthalamic nucleus (STN), subject #3 - 32 years old male, two epidural electrode strips implanted unilaterally (3240, St. Jude Medical Inc., USA) over the right motor cortex. Each electrode contained four recording points separated by 1.5mm (DBS) and 10mm (epidural), resulting in 8 channels. All subjects signed a written consent form and experimental protocol was approved by Ethics committee of Institute of Psychiatry of Hospital das Clinicas of University of São Paulo with the code 0636/09. All subjects were stimulated with tDCS using O2-supraorbital (EEG 10-20) montage, 5x7 cm electrodes for ~30 seconds with current ranging from 0-2 mA, in 1 mA increments. The voltage on each of the 8 electrodes in each subject was recorded during tDCS with reference to right earlobe at a sampling rate of 1200 Hz using a g.USBamp biosignal amplifier (g.tec, Austria). A standard head model (S#) was used to predict voltage distribution with aforementioned stimulation montage (Fig. 1). A standard set of electrical properties of tissue were assigned (in S/m): skin=0.456, fat=0.025, skull=0.01, CSF=1.65, grey matter=0.276, white matter=0.126, air=10^{-}-15, electrode=5.8*10^{-}7 and gel=1.4 [1, 5]. For modified conductivity, all parameters were fixed except for the grey matter=0.207 S/m and white matter=0.0945 S/m. Simulated voltages in locations corresponding to the center of each epidural electrode based on subject's CT scan were used to evaluate cortical model predictions. In DBS modeling, averaged voltages in segmented subcortical nuclei (i.e. NA, STN) were used for model evaluation due to imprecise estimate of DBS electrode locations inside nuclei (i.e., no CT scan after surgery in DBS-implanted subjects).

3. Results

Reliable voltages were recorded from epidural electrodes and DBS leads during DC stimulation that were linear with applied current intensity (Fig. 2). Epidural voltage recordings over the motor cortex were monotonic with distance from the anode (Fig. 2, C) reflecting semi-parallel direction of implanted motor strip relative to tDCS current flow (Fig. 1, B.3). Averaged voltage recording during ~30 second of stimulation for each intensity was used to assess model predictions at the corresponding positions (Table 1). Cortical data indicates that tDCS model predictions based on a standard head with standard conductivities are accurate ($V_{recording}$-V_{model})/$V_{recording}$ *100 < 30%). Even a significant change in grey/white matter conductivity had little influence on model precision. In contrast, modification of grey/white matter conductivity had relatively large effects on voltages predicted in sub-cortical structures (Table 1).

4. Discussion and Conclusion

In sum, our data indicates that tDCS model predictions based on a standard head and standard conductivities are accurate for cortical target areas. On the other hand, the voltage difference measured with DBS leads were smaller due to the closer inter-electrode distance and alignment of electrodes being perpendicular to tDCS current flow. Combined with the sensitivity of model prediction to local tissue conductivity (i.e., knowing the tissue conductivity of each nuclei and the precise position of each DBS electrode), subcortical tDCS voltages could not be validated reliably. However, our results are broadly consistent with conventional tDCS montages producing deep brain currents. Semi-parallel orientation of epidural electrodes relative to tDCS current flow led to monotonic changes in voltage measurement over motor cortex that could accurately validate model predictions in cortical region. We note this modeling was based on a standard head model anatomy rather than individualized models derived from the anatomical MRI of each of the study subjects, and moreover that predictions at the cortical surface were not especially sensitive to brain conductivity. In conclusion, our results based on a small data set: 1) are consistent with tDCS producing intra-cranial electric fields (0.1 V/m), that approximate electric fields reported functional in animal studies (0.2 V/m); and 2) suggest a standard head model and conductivities may produce a reasonable estimate of brain current flow.

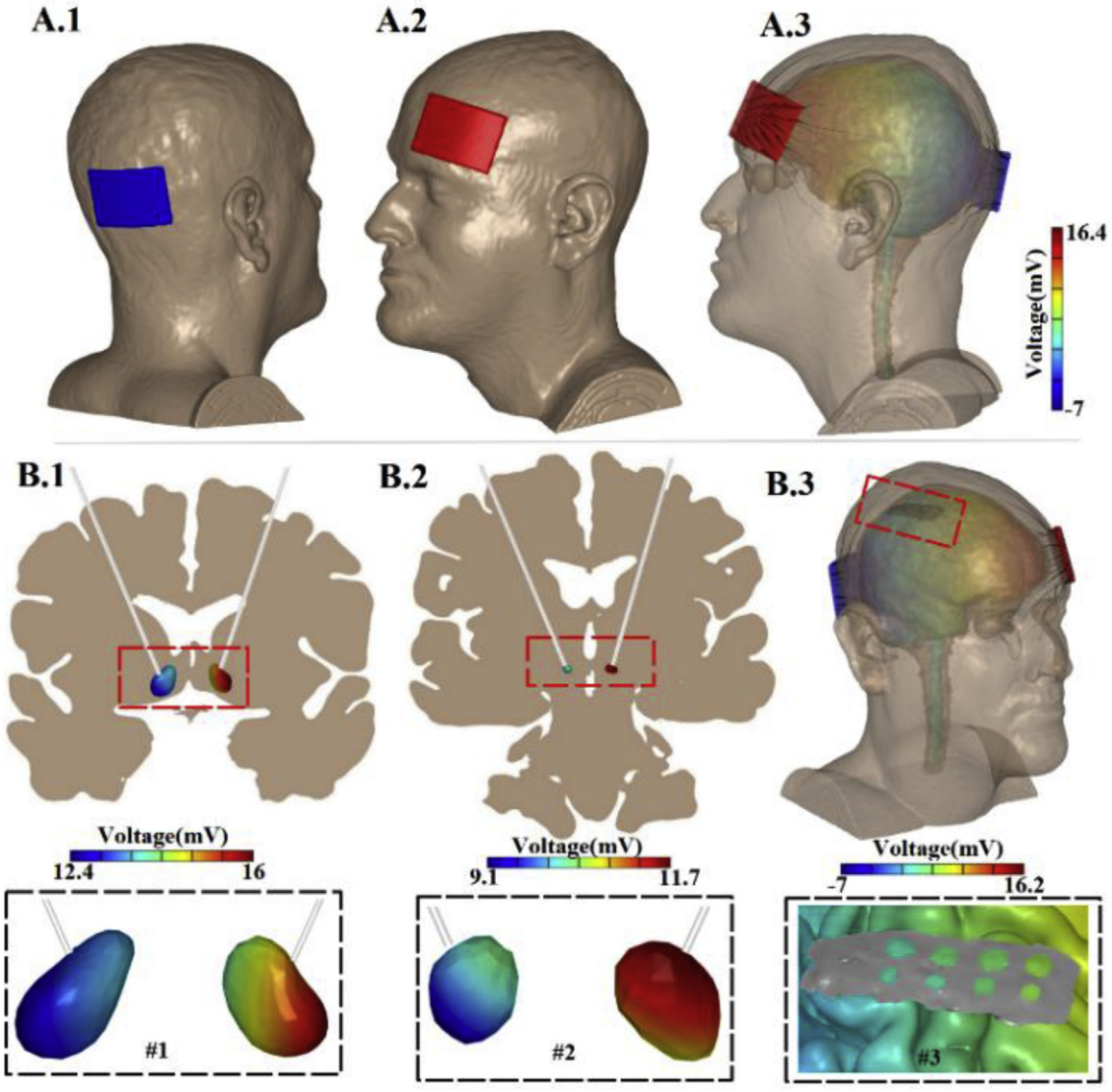

Fig. 1. High-resolution model using O2-Supraorbital montage (A.1, A.2) and resulting cortical voltage distribution for standard conductivity values and 1 mA stimulation (A.3). red: anode electrode; blue: cathode electrode. Simulated voltage (right earlobe refrenced) using standard conductivity values is highlighted in three recording sites (B.1: bilateral nucleus accumbence, 2 mA current intensity; B.2: bilateral subthalamic nuclei, 2 mA current intensity; B.3: epidural electrode implanted over right motor cortex, 1 mA current intensity).

Table 1
Summary of recorded voltages in each of 8 electrodes for all three subjects compared to model predictions in associated electrode locations.

Electrodes	Subjects								
	Subject #1 (Recording site= bilateral NA)			Subject #2 (Recording site=bilateral STN)			Subject #3 (Recording site=right motor cortex)		
	tDCS=2 mA			tDCS=2 mA			tDCS=1 mA		
	Voltage recording(mV)	Model prediction(mV)		Voltage recording(mV)	Model prediction(mV)		Voltage recording(mV)/ Estimated EF(V/m)	Model prediction(mV)/Estimated EF(V/m)	
		*	**		*	**		*	**
1	29.0	15.0	16.7	24.9	11.2	12.6	5.20/–	5.89/–	6.20/–
2	29.0	15.0	16.7	25.1	11.2	12.6	4.40/0.080	4.99/0.090	5.28/0.092
3	29.0	15.0	16.7	24.7	11.2	12.6	3.30/0.110	4.05/0.094	4.37/0.091
4	29.0	15.0	16.7	20.8	11.2	12.6	2.50/0.080	3.26/0.079	3.05/0.132
5	21.4	13.0	14.6	23.6	9.8	11.1	5.20/–	5.66/–	6.01/–
6	21.6	13.0	14.6	23.5	9.8	11.1	4.50/0.070	4.70/0.096	4.96/0.105
7	19.5	13.0	14.6	23.4	9.8	11.1	3.90/0.060	3.68/0.102	3.70/0.126
8	20.7	13.0	14.6	23.0	9.8	11.1	2.70/0.120	2.87/0.081	2.74/0.096

* Standard conductivity values

** Conductivity of both grey and white matter reduced to 75% of standard. Estimated electric field (EF) = (V2-V1)/d, d= 10 mm (Center to center distance between adjacent electrodes).

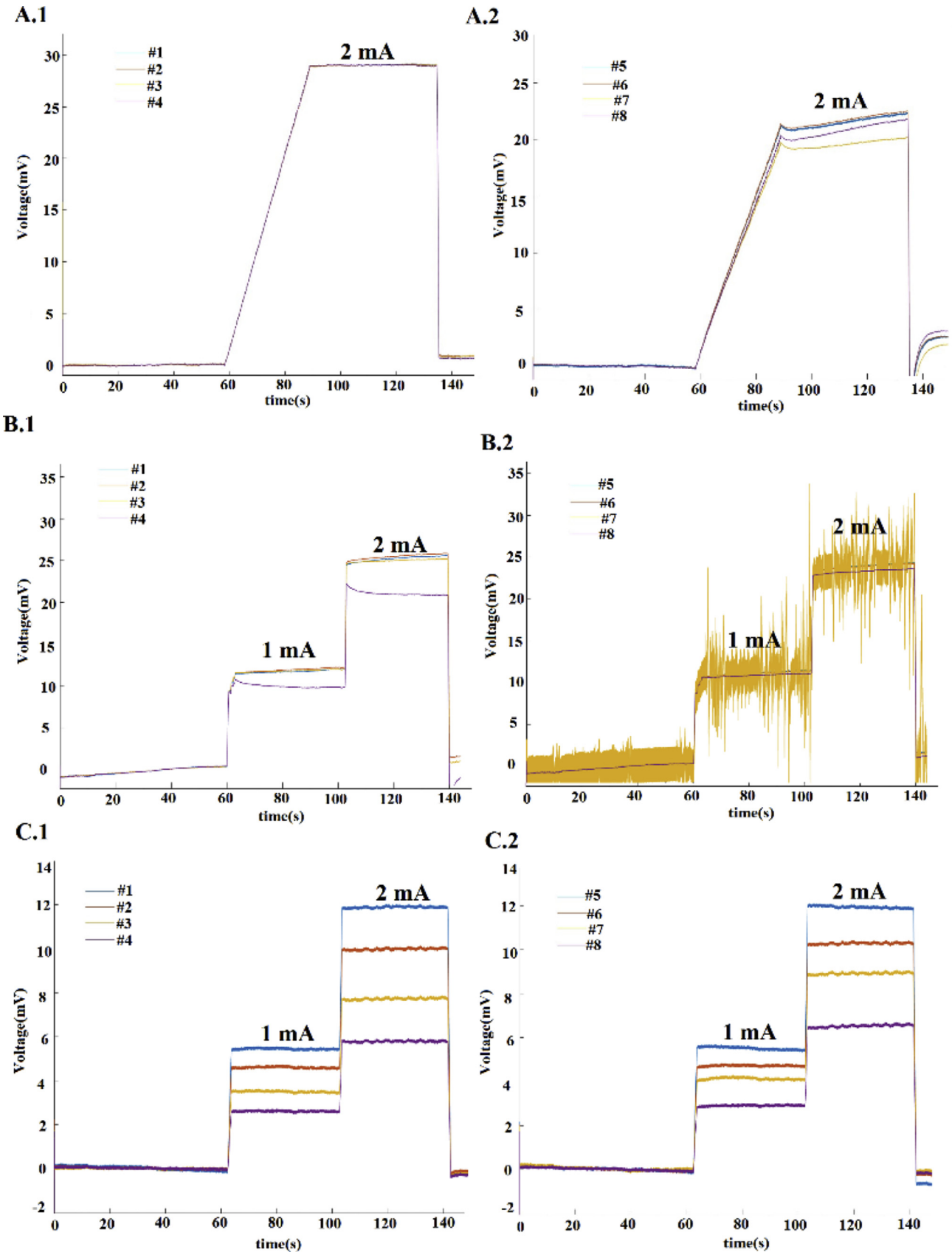

Fig. 2. Intra-cranial (epidural or DBS) voltage recordings during tDCS for three subjects. A. Voltage recordings from bilateral DBS leads implanted near nucleus accumbens in subject #1 during 2 mA tDCS. A.1: left, lead 1, electrodes 1-4 (most inferior to superior), A.2: right, lead 2, electrodes 5-8 (most inferior to superior). B. Voltage recordings from bilateral DBS leads implanted in the STN in subject #2 during 1 and 2 mA tDCS. B.1: left, lead 1, electrodes 1-4 (most inferior to superior). B.2: right, lead 2, electrodes 5-8 (most inferior to superior). C. Voltage recordings from epidural electrodes implanted over right motor cortex in subject #3 during 1 and 2 mA tDCS. C.1: medial, trip 1, electrodes 1-4 (most anterior to posterior). C.2: lateral, strip 2, electrodes 5-8 (most anterior to posterior).

References:

1. Kuo, M.-F., W. Paulus, and M.A. Nitsche, Therapeutic effects of non-invasive brain stimulation with direct currents (tDCS) in neuropsychiatric diseases. Neuroimage, 2014. 85: p. 948-960.
2. Reato, D., et al., Low-intensity electrical stimulation affects network dynamics by modulating population rate and spike timing. The Journal of Neuroscience, 2010. 30(45): p. 15067-15079.
3. Fritsch, B., et al., Direct current stimulation promotes BDNF-dependent synaptic plasticity: potential implications for motor learning. Neuron, 2010. 66(2): p. 198-204.
4. Datta, A., et al., Gyri-precise head model of transcranial direct current stimulation: improved spatial focality using a ring electrode versus conventional rectangular pad. Brain stimulation, 2009. 2(4): p. 201-207. e1.
5. Bikson, M., A. Rahman, and A. Datta, Computational models of transcranial direct current stimulation. Clinical EEG and Neuroscience, 2012. 43(3): p. 176-183.
6. Truong, D.Q., et al., Computational modeling of transcranial direct current stimulation (tDCS) in obesity: impact of head fat and dose guidelines. NeuroImage: Clinical, 2013. 2: p. 759-766.
7. Alam, M., et al., Spatial and polarity precision of concentric high-definition transcranial direct current stimulation (HD-tDCS). Physics in Medicine and Biology, 2016. 61(12): p. 4506.
8. Seibt, O., et al., The pursuit of DLPFC: non-neuronavigated methods to target the left dorsolateral pre-frontal cortex with symmetric bicephalic transcranial direct current stimulation (tDCS). Brain stimulation, 2015. 8(3): p. 590-602.
9. Datta, A., et al., Validation of finite element model of transcranial electrical stimulation using scalp potentials: implications for clinical dose. Journal of neural engineering, 2013. 10(3): p. 036018.
10. Edwards, D., et al., Physiological and modeling evidence for focal transcranial electrical brain stimulation in humans: a basis for high-definition tDCS. Neuroimage, 2013. 74: p. 266-275.
11. Opitz, A., et al., Spatiotemporal structure of intracranial electric fields induced by transcranial electric stimulation in human and nonhuman primates. bioRxiv, 2016: p. 053892.
12. Huange, Y., et al., Measurements and models of electric fields in the in vivo human brain during transcranial electric stimulation. eLife, 2016,in revision.

PROCEEDINGS #22. ANODAL TRANSCRANIAL DIRECT CURRENT STIMULATION INCREASES CEREBRAL BLOOD FLOW, TISSUE OXYGENATION AND IMPROVES NEUROLOGIC OUTCOME IN MICE AFTER TRAUMATIC BRAIN INJURY

Olga A. Bragina [1], Devon A. Lara [1], Yirong Yang [2], Edwin E. Nemoto [1], Claude W. Shuttleworth [3], Oxana V. Semyachkina-Glushkovskaya [4], Denis E. Bragin*[1]. [1] *Department of Neurosurgery, University of New Mexico School of Medicine, United States;* [2] *College of Pharmacy, University of New Mexico, United States;* [3] *Department of Neurosciences, University of New Mexico School of Medicine, United States;* [4] *Saratov State University, United States*

1. Abstract

Traumatic brain injury (TBI) causes neurologic deficit in 70% of survivors without a clinically effective therapy. Transcranial direct current stimulation (tDCS) is a prospective adjunct therapy for TBI but due to limited animal studies the mechanisms and optimal parameters are unknown. In this pilot study we examined the effects of repetitive anodal tDCS on cerebral blood flow (CBF) and brain oxygenation after TBI in mice and evaluated the efficacy in long-term neurologic recovery. Using *in-vivo* 2-photon laser scanning microscopy (2PLSM) we have shown that tDCS (0.1 mA/15min) improved microvascular CBF and tissue oxygenation in the pericontusional cortex in the recovery period after TBI, which was confirmed by global CBF by magnetic resonance imaging (MRI). Repetitive tDCS (4 weeks, 4 days/ week) significantly improved motor and cognitive neurologic outcome. tDCS acutely increases CBF and tissue oxygenation and contributes to improved neurologic recovery after TBI.

2. Introduction

Traumatic brain injury (TBI) is a major cause of death and long-term neurological disabilities in survivors [1]. The primary injury is followed by a secondary injury and pathophysiological cascades that persist for weeks to months after injury which may provide a wide time window for the treatment. Unfortunately, no effective therapies have not yet been proved for TBI [2].

Transcranial direct current stimulation (tDCS) is an emerging electrical neuromodulation technique that has been proposed for TBI treatment [3] but mechanisms and optimal stimulation parameters have not yet been determined due to lack of pre-clinical studies. Here we have examined the effect of repetitive anodal tDCS on-long term neurologic outcome in a mouse model of TBI and have tested the acute effects on CBF and oxygenation of the mouse brain in the recovery phase after TBI.

3. Methods

Animal studies were done according the NIH Guide for the Care and Use of Laboratory Animals; protocol approved by the Institutional Animal Care and Use Committee of the UNM. Four groups of 10 mice each was used in the study: TBI and Sham with and without stimulation. TBI was induced by a Benchmark Controlled Cortical Stereotaxic Impactor using a 3 mm flat-tip impounder deployed at a velocity of 5m/sec and depth of 2.0 mm from the cortical surface. Sham-controls subjected to craniotomy only. Repetitive tDCS (0.1 mA/15min) or Sham stimulation was done under anesthesia over 4 weeks for 4 consecutive days at 3-day intervals starting 3 weeks after TBI. The anode was placed around the craniotomy and the counter electrode on the thorax.

Cortical microvascular tone, cerebral blood flow (mCBF) and tissue oxygenation (NADH autofluorescence) were measured pre and post stimulation by 2PLSM and global CBF by arterial spin labeling MRI.

At one week after the end of stimulation, neurologic recovery was evaluated by a battery of behavioral tests: rotarod for sensory-motor deficits; passive avoidance for learning and memory and Y-maze for spatial memory.

The statistical analysis was done by independent Student's t-test or Kolmogorov-Smirnov tests where appropriate. Differences between groups were determined using two-way repeated measures (ANOVA) for multiple comparisons and post hoc testing using the Mann–Whitney U-test using GraphPad Prism (GraphPad Software, Inc., La Jolla, CA). Statistical significance level was set at $P<0.05$. Data are presented as mean ± SEM.

4. Results

CCI-induced moderate TBI caused tissue damage in the cortex and subcortical zones including hippocampus in the ipsilateral hemisphere as shown by T2 anatomical MRI and H&E staining. Nissl staining revealed a shrunken hippocampus and obvious shrinkage of parietal somatosensory cortex with 18% counted neuronal loss compared to the contralateral hemisphere.

TBI impaired motor and coordination functions as shown using rotarod test by a decrease in latency period to fall from a rotating rod compared to sham-injured animals (Fig. 1A, $P<0.001$). Repetitive tDCS attenuated motor deficit; latency to fall in stimulated group was longer than in a sham-stimulated group (Fig. 1, 114.6 ± 21.5 vs. 78.8 ± 12.5 sec., $p<0.05$).

Passive avoidance test revealed impaired learning and memory in traumatized mice (Fig. 1B, $P<0.001$). This is a fear-motivated avoidance task in which the mouse learns to refrain from stepping through a door to an apparently safer but previously punished dark compartment. The latency to refrain from crossing into the punished compartment serves as an index of the ability to avoid, and allows memory to be assessed. In the tDCS TBI group learning and memory were better preserved; step-through retention latency was significantly longer ($P<0.01$) than that of sham-stimulated mice (Fig. 1B, 326.3 ± 68.1 vs. 130.5 ± 60.9 sec., respectively). Interestingly in sham operated mice, the tDCS group performed better than sham-stimulated, $P<0.05$.

Y-maze assesses spatial working memory using the natural inclination of mice to explore new regions of their environment. Sham-operated animals spent most of the time exploring new arm. TBI impaired spatial working memory as they spent time evenly in all three arms (Fig. 1C, $P<0.01$). tDCS-stimulated mice entered in to the new-opened arm more frequently compared to sham-stimulated (Fig. 1C, $P<0.05$). In the sham-operated group stimulation also significantly enhanced spatial working memory (Fig. 1C, $P<0.05$).